

Carbon Quantum Dots with Photoenhanced Hydrogen-Bond Catalytic Activity in Aldol Condensations

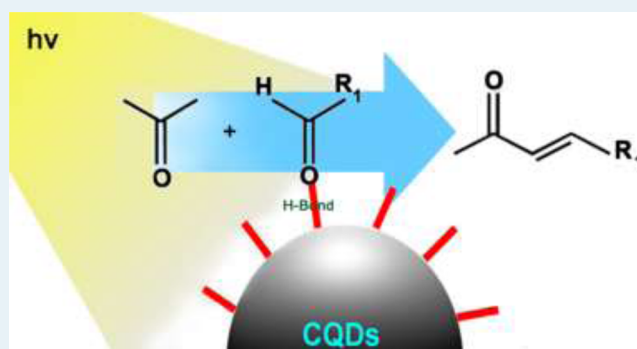
Yuzhi Han, Hui Huang, Hengchao Zhang, Yang Liu,* Xiao Han, Ruihua Liu, Haitao Li, and Zhenhui Kang*

Institute of Functional Nano & Soft Materials (FUNSOM) and Collaborative Innovation Center of Suzhou Nano Science and Technology, Soochow University, Suzhou, Jiangsu 215123, China

Supporting Information

ABSTRACT: Carbon quantum dots (CQDs) were synthesized by an electrochemical etching method. The CQDs are well-dispersed with uniform size about 5 nm. FT-IR spectra suggest the presence of many hydroxyl groups on the surface of CQDs. Here, CQDs with diameter approximately 5 nm, directly used as effective heterogeneous nanocatalysts for H-bond catalysis in aldol condensations, show excellent photoenhanced catalytic ability (89% yields when 4-cyanobenzaldehyde is used). It demonstrated that aldol condensation between acetone and aromatic aldehydes resulted in higher yields with visible light irradiation than in the dark, confirming visible light is necessary for good conversion. The H-bond catalytic activities of CQDs can be significantly enhanced with visible light irradiation. The high catalytic activities of CQDs are due to highly efficient electron-accepting capabilities. Repeated catalytic experiments suggest that the CQD catalyst can be easily recycled as a heterogeneous catalyst with a long catalyst life.

KEYWORDS: carbon quantum dots, hydrogen bond catalysis, heterogeneous catalysis, aldol condensation, electron acceptor/donor



Hydrogen bonding (H-bonding) plays a crucial role in enzyme-catalyzed reactions by orienting the substrate molecules and lowering barriers to reactions.¹ Recently, this kind of noncovalent interaction (H-bonding) was introduced into many organic chemical reactions,^{2–9} including the Diels–Alder, Aldol reaction, aza-Henry, Mannich, Michael, Morita–Baylis–Hillman, and Strecker reactions.^{10–17} As a typical organocatalysis, hydrogen bond (H-bond) catalysis uses H-bonding interactions to accelerate organic reactions and stabilize anionic intermediates and transition states.¹⁸ Several organic molecules with hydroxyl groups can be used as homogeneous H-bond catalysts.^{19–21} For example, Chiral BINOL-derived Brønsted acids catalyze the enantioselective, asymmetric Morita–Baylis–Hillman (MBH) reaction of cyclohexenone with aldehydes.²² However, these catalytic reactions produce low yields, and it is difficult to isolate the catalyst from the reaction system. Inorganic solid nanoparticles with abundant surface hydroxyl groups have been developed as alternative heterogeneous catalysts for H-bonding reactions.^{23,24} For example, aldol reactions could be catalyzed by hydroxyl groups on the Fe(OH)₃ shell of Fe₃O₄@Fe(OH)₃ core–shell microspheres.²⁵ However, compared with a bioenzyme system, this artificial catalyst system faces the challenges of low efficiency and poor controllability.

Carbon quantum dots (CQDs) constitute a new class of zero-dimensional nanostructures with sizes below 10 nm.²⁶ As a novel class of recently discovered nanocarbons, CQDs are

stable and biocompatible and have strong and tunable photoluminescence (PL). In addition to downconverted PL, CQDs show excellent up-converted PL (UCPL), which enable CQDs to efficiently utilize the full spectrum of sunlight.²⁷ Due to the novel PL and excellent photoinduced electron transfer/reservoir properties of CQDs, composites of CQDs and semiconductors have been successfully prepared. CQD/semiconductor composites have enhanced photocatalytic activities and are stable in visible light. Examples include CQDs/TiO₂, CQDs/SiO₂, CQDs/Fe₂O₃, CQDs/Cu₂O, and CQDs/Ag₃PO₄.^{26–30} CQDs are considered to be good H-bonding catalysts because of their rich photochemical properties and functional carboxylic and hydroxyl groups.

In the current study, we used CQDs as heterogeneous nanocatalysts for H-bond catalysis. CQDs showed good photoenhanced catalytic abilities (89% yield when 4-cyanobenzaldehyde is used) in the aldol condensation. A series of catalytic experiments confirmed that the catalytic activity of CQDs can be effectively enhanced by visible light, which may be attributed to their photoinduced electron-accepting properties.

CQDs were synthesized through an electrochemical etching method (see the experimental section in the Supporting

Received: August 14, 2013

Revised: January 21, 2014

Published: January 26, 2014

Information (SI)).²⁸ A typical transmission electron microscopy (TEM) image of the as-synthesized CQDs is shown in Figure 1a. The CQDs were well-dispersed and uniform with

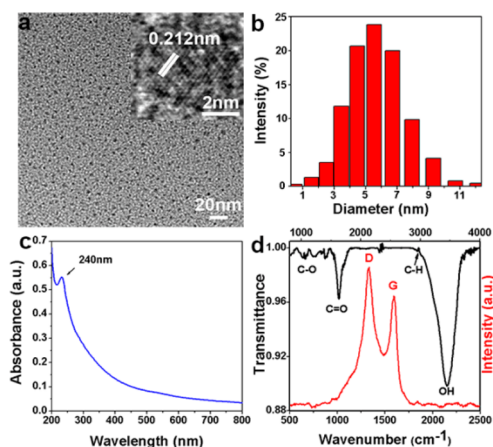


Figure 1. (a) TEM image of CQDs (inset is HRTEM image), (b) particle-size histogram, (c) UV–vis absorption spectrum, (d) Raman (red line) and FT-IR (black line) spectra of 5 nm CQDs.

diameters of about 5 nm. A high-resolution TEM (HRTEM) image of the CQDs (Figure 1a inset) shows that the lattice spacing was around 0.212 nm, which is consistent with the (100) facet of the graphite. The size distribution (Figure 1b) was calculated by measuring approximately 200 particles. The CQDs had an average size of 5.40 ± 0.72 nm.

A typical CQD ultraviolet and visible (UV–vis) absorption spectrum was shown in Figure 1c. The peak at 240 nm represented the typical absorption of an aromatic π system, which is similar to that of polycyclic aromatic hydrocarbons. CQDs showed broad absorption of sunlight in the ultraviolet and visible region, which suggested that CQDs may have high photocatalytic activities in visible light. Raman and Fourier transform infrared (FT-IR) spectra were recorded to provide further structural insights about the as-synthesized CQDs. The Raman spectrum of CQDs showed two characteristic peaks at about 1330 and 1595 cm^{-1} (Figure 1d, red line), which corresponded to the D-band and G-band of carbon, respectively. The peak at 1330 cm^{-1} (D-band) was associated with the vibrations of sp^3 -banded carbon atoms in disordered graphite. The peak at 1595 cm^{-1} (G-band) corresponded to the vibrations of sp^2 carbon atoms in a two-dimensional (2D) hexagonal lattice. The FT-IR spectrum (Figure 1d, black line) showed a broad peak centered at 3445 cm^{-1} , which suggested the presence of many hydroxyl groups on the CQD surface. The peak at about 2960 cm^{-1} corresponded to the C–H stretch of polycyclic aromatic hydrocarbons. The peaks at about 1637 cm^{-1} and in the range of 1000–1400 cm^{-1} indicated the presence of carbonyl (C=O) and C–O groups, respectively. The TEM images, HRTEM images, particle-size histograms, UV–vis absorption, Raman (red line), and FT-IR (black line) spectra of CQDs (<4 nm and >10 nm) were shown in Figures S1 and S2, respectively. The energy dispersive X-ray spectroscopy (EDS) analysis of four kinds of CQDs were shown in Figure S6. Figure S7 provided the pictures of solid CQDs (<4 nm; 5 nm; >10 nm and hydroxyl-group-free CQDs), indicating that these CQDs can well-dissolved in solvent.

To further explore the optical properties of as-synthesized CQDs, a detailed PL investigation was carried out with different

excitation wavelengths in the same sample. Figure S3 shows the PL spectra of the as-synthesized CQDs with different sizes: (a) <4 nm; (b) 5 nm; and (c) >10 nm. The excitation wavelength of the black, red, blue, green, magenta, and dark yellow PL lines are 240, 300, 360, 420, 500, and 580 nm, respectively. The PL spectra show that the as-synthesized CQDs with different sizes exhibit the different distribution of emission colors, and that smaller size (<4 nm) leads to increasing amount of CQDs emitting at shorter wavelengths.


The CQDs (5 nm) without surface hydroxyl groups were synthesized for comparison (the detailed experiments are in SI). Figure S4a shows the typical TEM image of hydroxyl-group-free CQDs. The CQDs are well-dispersed and uniform with diameter of about 5 nm. The inset in Figure S4a is the EDS analysis of hydroxyl-group-free CQDs. No N signal was detected, indicating that the amines do not exist in reaction system. Elemental analyses of C, N, O, and H were further performed with an Elementar Vario EL III elemental analyzer (shown in Table S2). The results show that only carbon, hydrogen, and oxygen elements were observed with no additional elements on the CQDs. These results indicate that the catalytic active sites are the oxygen functional groups on the surface of CQDs. The size distribution (Figure S4b) was calculated by measuring approximately 200 particles, revealing that the CQDs have an average size of 5.00 ± 0.58 nm. The typical CQD UV–vis absorption and PL spectra were shown in Figure S4c. The peak at 240 nm represented the typical absorption of an aromatic π system. Furthermore, the CQDs revealed broad absorption of sunlight in the ultraviolet and visible region. The PL spectrum shows that the maximum emission wavelength of the hydroxyl-group-free CQDs aqueous solution is 504 nm. FT-IR spectrum was recorded to provide further structural insights about the hydroxyl-group-free CQDs (Figure S4d). Compared with Figure 1b, which shows the presence of many hydroxyl groups on the water-soluble CQD surface, this spectrum indicated a narrow and weak peak centered at 3443 cm^{-1} , suggesting a small amount of hydroxyl groups on the surface of hydroxyl-group-free CQDs. This can explain why hydroxyl-group-free CQDs cannot catalyze the reaction but water-soluble CQDs can. The peaks at about 1635 cm^{-1} and in the range of 1000–1400 cm^{-1} indicated the presence of carbonyl (C=O) and C–O groups, respectively.

To quantify the hydroxyls and carboxylic acid on the surface of the water-soluble CQDs (about 5 nm), base titration was performed to measure the total quantity of both hydroxyls and carboxylic acid following a standard method.^{31a} Subsequently, the relative content of hydroxyls versus carboxylic acid of the water-soluble CQDs (about 10:1) was determined by conductometric titration (for experimental details, see SI and Figure S5).^{31b} The detailed quantification data were shown in Table S1.

The photoenhanced catalytic activities of CQDs (about 5 nm) were confirmed in the Aldol reaction, which is an important strategy for C–C bond formation in organic synthesis.^{31c} Song and co-workers showed that the Aldol reaction between aromatic aldehydes and ketone in solvent (acetone, ethanol, THF, CHCl_3) can proceed and the aldol condensation products can be gained directly.²⁵ Herein we report aldol condensation with a high yield of the aldol condensation product under CQDs as catalyst. In our experiments, acetone was the solvent and reactant in the first set of trials and reacted with a series of aromatic aldehydes at room temperature. Detailed yields of the aromatic compounds

are displayed in Table 1. As shown in entry 8, the aldol condensation exhibited a very low yield in the absence of

Table 1. Room-Temperature Aldol Condensation between Acetone and Aromatic Aldehydes in the Presence of CQDs with or without Visible Light



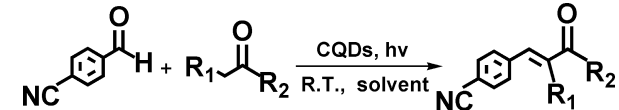
entry ^a	Ar-	light ^b		dark ^b	
		yields (%) ^c		yields (%)	
1	C ₆ H ₅	19	3		
2	4-Cl-C ₆ H ₄	68	15		
3	4-Br-C ₆ H ₄	63	13		
4	4-NO ₂ -C ₆ H ₄	65	8		
5	4-CN-C ₆ H ₄	89	18		
6	4-CH ₃ -C ₆ H ₄	67	9		
7	4-CH ₃ O-C ₆ H ₄	65	8		
8 ^d	4-CN-C ₆ H ₄	trace	trace		
9 ^e	4-CN-C ₆ H ₄	99	32		

^aReaction conditions: 0.2 mmol aromatic aldehydes, 2 mL acetone, 60 mg CQDs, room temperature, 24 h. ^bReference experiments with and without visible light irradiation, respectively (Xenon lamp, 300 W, $\lambda \geq 420$ nm). ^cThe reaction products were isolated through silica column chromatography and analyzed by GC. ^dReference experiment without catalyst. ^eHeated to 50 °C, 4h.

CQDs as catalysts whether under light irradiation or not, confirming the CQDs as catalyst is necessary for the reaction. In general, these reactions yielded higher yields with visible light irradiation than those produced in the dark. These data confirm that visible light is necessary for good conversion. When benzaldehyde (entry 1) is used, the lowest yield in visible light (19%) with CQDs as catalyst (Table 1) was obtained. Other aromatic aldehydes (Table 1, entries 2–7) showed higher conversion. Among them, when 4-cyanobenzaldehyde is used, the aldol condensation showed the highest yield (89%, entry 5) with CQDs as catalyst. These catalytic results were similar to the results reported by Song et al.²⁵ It would be attributed to the weak interaction between the para-position of aldehyde group and the groups on the CQDs surface, which make the reactant molecules closer to the catalytic active center. In contrast, without visible light irradiation, yields were reduced to 18% for 4-cyanobenzaldehyde (entry 5). When the reaction temperature was elevated to 50 °C, a total conversion of 4-cyanobenzaldehyde in aldol condensation was achieved in 4 h (Table 1, entry 9). When 4-chlorobenzaldehyde (entry 2) and 4-bromobenzaldehyde (entry 3) were used, the yields reached 68% and 63%, respectively, with visible light irradiation, whereas the yields fell to 15% and 13% in the dark. In the present system, the reaction products were dehydrated products, and the typical one (Table 1, entry 1) was (*E*)-4-phenylbut-3-en-2-one (analyzed by gas chromatography (GC) and H nuclear magnetic resonance spectroscopy (HNMR), shown in Figures S8 and S9).

In the following experiments, different solvents (toluene, ethanol, THF, and CHCl₃) and ketones (cyclopentanone, cyclohexanone, and acetone) were selected to evaluate the catalytic abilities of CQDs (about 5 nm) for aldol condensations with 4-cyanobenzaldehyde. The corresponding aldol condensations shown in Table 2 were performed with and without visible light at room temperature. On the whole, in the

Table 2. Aldol Condensation between 4-Cyanobenzaldehyde and Ketones in Various Solvents Catalyzed by CQDs with or without Visible Light Irradiation



entry ^a	ketone/solvent	light ^b		dark	
		yields (%) ^c		yields (%)	
1	acetone/ethanol	23	trace		
2	acetone/THF	32	trace		
3	acetone/CHCl ₃	12	trace		
4	cyclopentanone/toluene	67	trace		
5	cyclohexanone/toluene	54	trace		

^aReaction conditions: 0.2 mmol 4-cyanobenzaldehyde, 1 mmol ketones, 2 mL solvent, 60 mg CQDs, room temperature, 24 h. ^bVisible light irradiation (Xenon lamp, 300 W, $\lambda \geq 420$ nm). ^cAnalyzed by GC analysis.

absence of light, nearly no conversion was observed. In contrast, high yields were simultaneously achieved with visible light irradiation (Table 2, entries 1–5). A series of catalytic experiments with the same reactant and different solvents (Table 2, entries 1–3) indicated that solvents greatly influenced the CQD-catalyzed aldol condensation. As shown in Table 2, when ethanol (entry 1), THF (entry 2), and CHCl₃ (entry 3) were used as solvents, the highest yield when 4-cyanobenzaldehyde was used (32%) was obtained with THF as solvent. The lowest yield (12%) was for CHCl₃. Different ketones were also tested with toluene as the solvent (Table 2, entries 4–5). When cyclopentanone (entry 4) and cyclohexanone (entry 5) were used, aldol condensations showed yields of 67% and 54%, respectively. These data suggest that different ketones influence the aldol condensation. In contrast, a higher yield of 89% was obtained when acetone was the solvent and reactant (Table 1, entry 5). Thus, in the present catalytic system, toluene was the most suitable solvent for the aldol condensation with CQDs as catalysts.

All of the above experimental results demonstrate that CQDs are excellent photocatalysts for the aldol condensation. Considering that these reactions were performed at room temperature, it is unlikely that cationic or anionic intermediates formed in these CQD-catalyzed reactions. However, the hydroxyl groups on the surface of CQDs are very weak acids, which can form H-bonds with oxygenates.^{32,33} Therefore, we propose that H-bonds catalyzed the aldol condensations in the present system.

Both reactants (aldehydes and ketones) are able to form H-bonds in the aldol condensation with CQDs as catalysts. We demonstrated that the hydroxyl groups on the surface of CQDs prefer to contact aldehyde groups. In a control experiment, 0.01 mmol 4-cyanobenzaldehyde, 0.01 mmol acetone, (aldehyde/ketone, molar ratio = 1:1), and 60 mg 5 nm CQDs were mixed with 1 mL *p*-xylene and stirred for 10 min followed by centrifugation to obtain a clear solution. The solution was analyzed by GC to determine the relative content of 4-cyanobenzaldehyde versus acetone in the solution. GC analysis showed that the molar ratio of aldehyde/ketone decreased to 1:2 after mixing with 5 nm CQDs. As shown in Table S4, there was no change in molar ratio when no catalyst was used, but the molar ratios of aldehyde/ketone decreased to 1:1.7, 1:2.0, and 1:1.6 when <4 nm, 5 nm, and >10 nm CQDs were used,

respectively. These data support stronger H-bonding between 4-cyanobenzaldehyde and the catalyst versus the ketone and catalyst.

We further studied the reactions catalyzed by CQDs-OD (surface bound with -OD but not -OH) to prove that CQDs could improve the reactions' conversion via surface H-bond catalysis rather than acid catalysis. CQDs-OD were prepared by the electrochemical etching method in heavy water (D₂O). The aldol condensation between 4-cyanobenzaldehyde and acetone was catalyzed by CQDs-OD to produce products 1 and 2 (Table 3). If CQDs work as acid catalysts, the O-D

Table 3. H/D Exchange Results for the Aldol Condensation

entry ^a	catalyst	yields (%)		X (%) ^b
		light	dark	
1	CQDs-OD	75	17	0 ^c

^aReaction conditions: 0.2 mmol 4-cyanobenzaldehyde, 2 mL acetone, 60 mg CQDs-OD, room temperature, 24 h. ^bX = Deuterium content in products (atom %). ^cBased on the identical ion mass pattern of water.

bonds on their surfaces will be destroyed during H/D exchange and will form the deuterium-labeled products, D₂O or HDO. Deuterium signals were not detected in products 1 or 2 by GC-mass spectrometry (GC-MS) analyses (see Table 3), further proving that the reaction products were dehydrated products. In other words, CQDs act as H-bond catalysts in the aldol condensation. The O-D bonds form single or multiple H-bonds (D-H...O) with aldehyde to promote the aldol condensation, and then H-bonds open, demonstrating that the O-D bonds on CQDs-OD surfaces have not been destroyed. At last, CQDs-OD was separated via centrifugation from the reaction mixture.

CQDs without surface hydroxyl groups were synthesized for comparison. The same amounts of hydroxyl-group-free CQDs were then used as catalysts for the same reaction in the same conditions. Interestingly, hydroxyl-group-free CQDs were unreactive, and no product was detected with or without visible light irradiation. This dependence on a hydroxyl group suggests that the ability of CQDs to mediate reactions is via interfacial H-bond catalysis. As shown in Table S3, a series of controlled trials proved that phenol and oxalic acid have very low catalytic effect, indicating that weak acids almost cannot catalyze the aldol condensation between acetone and aromatic aldehydes.^{12b,32}

The Table 1 results (entry 5) revealed that the conversion of 4-cyanobenzaldehyde was about 4 times higher when the mixture was stirred under visible light versus when the reaction was performed in the dark. We compared the FT-IR spectra of benzaldehyde mixed with 5 nm CQDs before and after visible light irradiation to further investigate the catalytic mechanism. Figure 2 shows the FT-IR spectra in the O-H stretching region. As shown in the enlarged graph (inset in Figure 2), the peak around 3400 cm⁻¹ corresponded to the vibrations of O-H...O. A characteristic peak was observed at 3371 cm⁻¹ (black line) before visible light irradiation due to the presence of many hydroxyl groups on the CQD surface. Then the mixture was exposed to visible light for 10 min and was detected after

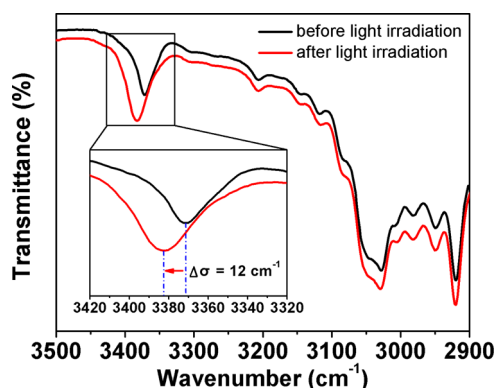


Figure 2. FT-IR spectra of benzaldehyde mixed with CQDs in the -OH stretching region (inset, enlarged graph corresponding to the black rectangle). The red and black curves denote the solutions tested after and before visible light irradiation, respectively. The peak positions of the curves are marked by vertical lines.

irradiation. As shown in the red line, the peak shifted to 3383 cm⁻¹. This is a blue-shift ($\Delta\sigma = 12 \text{ cm}^{-1}$, from 3371 cm⁻¹ to 3383 cm⁻¹), and the increase of frequency means the stretching vibration of O-H...O was enhanced,³⁴ suggesting that light enhanced the interaction between the functional group and aldehyde. So the H-bond catalytic activities of CQDs can be significantly enhanced with visible light irradiation, which is consistent with our experimental results shown in Tables 1 and 2. On the basis of these experimental results, we propose the following mechanism for the enhanced photocatalytic activity of CQD photocatalysts. CQDs can bind with aldehydes by H-bonding to form CQD-aldehyde complexes. CQDs act as highly efficient electron acceptors in visible light. Electrons transfer from the O-H...O region to part of the electron acceptor and lead to the blue-shift, suggesting that CQDs have highly enhanced photocatalytic activity for target reactions.^{35,41}

FT-IR spectra of 4-cyanobenzaldehyde mixed with three different sizes CQDs and hydroxyl-group-free CQDs (5 nm) before and after visible-light irradiation in the -OH stretching region were shown in Figure S11. As shown in Figure S11a, the black line is the FT-IR spectrum of 5 nm CQDs in the -OH stretching region. Blue and red line are for the mixture of 4-cyanobenzaldehyde and 5 nm CQDs before and after visible-light irradiation, respectively. The red shift (black line to blue line, $\Delta\sigma = 12 \text{ cm}^{-1}$) indicates the formation of hydrogen bond after adding 4-cyanobenzaldehyde.³⁶ Further exposing the mixture of 4-cyanobenzaldehyde and CQDs under visible light for 10 min and then the FT-IR spectrum (red line) was detected. The blue shift (blue line to red line, $\Delta\sigma = 21 \text{ cm}^{-1}$) proves that the H-bond catalytic activities of CQDs can be significantly enhanced with visible light irradiation.^{35,41} The similar results were obtained when >10 nm CQDs and <4 nm CQDs were tested. Figure S11b,c shows the FT-IR spectra of 4-cyanobenzaldehyde mixed with >10 nm CQDs and <4 nm CQDs before and after visible-light irradiation in the -OH stretching region, respectively. The red shifts for >10 nm CQDs and <4 nm CQDs were 8 and 3 cm⁻¹, respectively, when a hydrogen bond formed. Then, the blue shift (11 cm⁻¹ for >10 nm CQDs and 7 cm⁻¹ for <4 nm CQDs) were detected after visible light irradiation for 10 min. These blue shifts were smaller than that for 5 nm CQDs (21 cm⁻¹) due to the highly efficient electron accept ability of 5 nm CQDs. This was elucidated in the next experiments. The FT-IR spectra of 4-

cyanobenzaldehyde mixed with hydroxyl-group-free CQDs were shown in Figure S11d, which shows no shift whether the mixture was exposed under visible light or not, indicating that there is no hydrogen bond formation.

To elucidate the photoenhanced catalytic abilities of CQDs, the time-correlated single-photon counting (TCSPC) experiments were performed to verify the photoinduced electron-accepting properties of CQDs. The charge transfer of CQDs was tested in the presence or absence of electron donor *N,N*-diethylaniline (DEA, 0.88 V vs NHE)³⁷ and electron acceptor 2,4-dinitrotoluene (−0.9 V vs NHE).^{38,39} CQDs with three different average particle sizes (5 nm, >10 nm, and <4 nm) were tested. As shown in Figures 3a and S12a, the

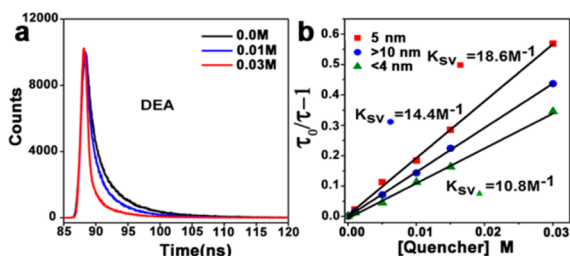


Figure 3. (a) Luminescence decays (485 nm excitation, monitored with 550 nm narrow bandpass filter) of the CQDs with DEA, (b) Stern–Volmer plots for the quenching of luminescence quantum yields (485 nm excitation) of the different-sized CQDs by DEA.

luminescence of CQDs was quenched by DEA and 2,4-dinitrotoluene. These results show that photoexcited CQDs are excellent electron donors and electron acceptors. The Stern–Volmer plots for the quenching of luminescence by DEA are shown for the different-sized CQDs in Figure 3b. The quenching constants ($K_{SV} = \tau_F k_q$) from linear regression were calculated to be 18.6 (5 nm CQDs), 14.4 (>10 nm CQDs), and 10.8 M^{-1} (<4 nm CQDs), respectively. The quenching constant for 2,4-dinitrotoluene was 14.5 M^{-1} (5 nm CQDs, Figure S12b). Obviously, the constant for DEA (18.6 M^{-1}) is larger than that of 2, 4-dinitrotoluene (14.5 M^{-1}), indicating that the as-synthesized CQDs (5 nm) are highly efficient electron acceptors. The Stern–Volmer plots for the quenching of luminescence quantum yields of the hydroxyl free CQDs by DEA and 2, 4-dinitrotoluene were shown in Figure S13.

Next, we performed the control experiments to study the influence of size on the photocatalytic activity of CQDs. The CQDs with three different average diameters (5 nm, >10 nm, and <4 nm) were used to catalyze the reaction between 4-cyanobenzaldehyde and ketones. The reaction yields were shown in Table 4. The highest yield of 89% was achieved for 5 nm CQDs when 4-cyanobenzaldehyde is used, whereas yields of 40% and 25% were obtained for CQDs >10 nm and <4 nm, respectively. Here, 5 nm CQDs had the most satisfying photocatalytic performance for this H-bond catalysis reaction, which should attribute to the highest electron-accepting ability when compared with other CQDs (with size >10 nm and <4 nm).

The rehybridization and hyperconjugation act in opposite directions, the effect of the bond lengths of H-bonding is a result of a balance of these two intrinsic effects. The O–H bond lengthens when hyperconjugation is dominant, and the O–H bond shortens when hyperconjugation is weak and the structure of the H-bond donor allows for a significant change

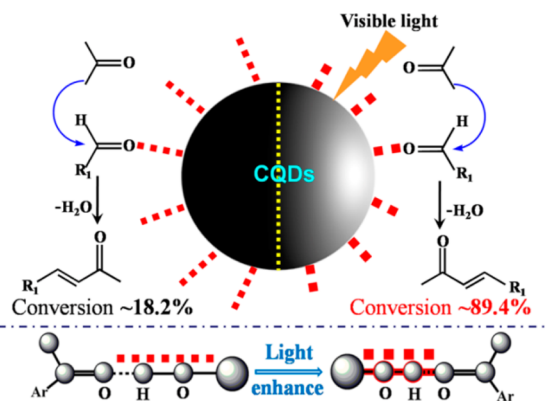
Table 4. Aldol Condensation between 4-Cyanobenzaldehyde and Ketones in Acetone Catalyzed by CQDs of Different Sizes^a

catalyst	size (nm)	<i>t</i> (h)	yields (%) ^b
CQDs	5	24	89
	>10	24	40
	<4	24	25

^aReaction conditions: 2 mL acetone, 0.2 mmol 4-cyanobenzaldehyde, 1 mmol ketones, 60 mg CQDs, room temperature, 24 h. ^bVisible light irradiation (Xenon lamp, 300 W, $\lambda \geq 420$ nm).

in O–H bond hybridization.⁴² The first O–H bond shortening effect is due to the increase in C–H bond polarization upon H-bond formation. The second group of changes involves O–H bond shortening effects. As shown in Scheme 1, the surface

Scheme 1. Schematic of the Photoenhanced Catalytic Mechanism of H-Bond Catalysis by CQDs in Visible Light



hydroxyl groups on the surface of CQDs form single or multiple H-bonds with 4-cyanobenzaldehyde. The CQD–aldehyde complex can be considered to be a reaction substrate for other molecules. H-bonds decreased the energy barrier for the reaction in the dark, and a lower 4-cyanobenzaldehyde yield of 18.2% was obtained. Our TCSPC experiments (Figure 3) proved that CQDs act as highly efficient electron acceptors with visible light irradiation, as these electron acceptors attract electrons from the O–H...O region. This effect results in the increase of positive charge on hydrogen and the increase of negative charge on oxygen. The group of changes is reflective of a decrease in effective electronegativity of the hydrogen atom which, in excellent agreement with Bent's rule, leads to an increase in the s-character in the oxygen hybrid orbital forming the O–H bond effect, thereby leading to O–H bond shortening.^{42,43} In other words, this process in turn leads to a strengthening of the O–H bond and effectively activates the C=O bond of 4-cyanobenzaldehyde and accelerates the aldol condensation. At the same time, the enhanced O–H bonds may further stabilize the reaction-intermediate species or transition-state species, which promote higher yields (highest yield of 89.4%).^{18,40}

Repeated catalytic experiments were performed by recycling the CQDs catalysts five times. It was found that the yields were almost the same in all five runs (Figure 4). When 5 nm CQDs

were used as catalysts, the yields for the first and fifth cycle were 89.4% and 82.6%, respectively.

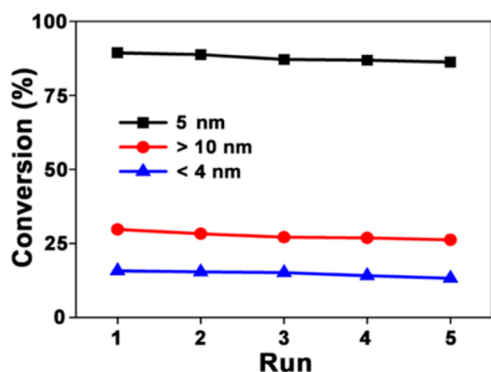


Figure 4. Recycling results for the different sizes of CQDs as catalysts (5 nm, >10 nm, and <4 nm) after five runs.

In order to further clarify the effect of light, the following experiments were carried out. We irradiated the mixture (solvent, 5 nm CQDs, and aldehyde) for 6 h and then removed the light source, and we monitored the conversion as a function of time. As shown in Figure 5, the black line shows the

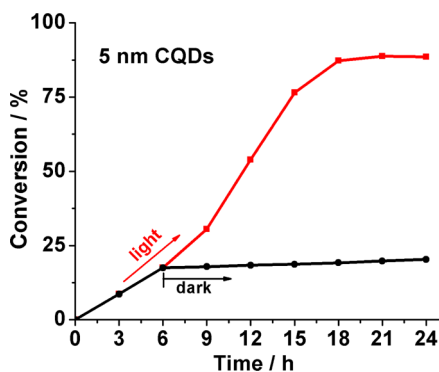


Figure 5. Kinetic plots monitor the conversion as a function of time (black line: exposed in the first 6 h and in the dark the next time; red line: exposed in light all the time).

conversion of the reaction, which was irradiated in the first 6 h and then kept in the dark. Compared with the red line (exposed in light all the time), the conversion (see black line) does not improve obviously after removing the light source, suggesting that the light is actually needed for photocatalytic enhancement activity.

The kinetic plots tracking yield over time for the first, second, and fifth cycle experiments are shown in Figure 6. These plots unambiguously demonstrate an induction period, which suggested that the most active catalytic species are not initially present. The reason is the CQD catalysts were initially not dispersed when we added to the reaction mixture. As shown in Figure 6a, when 5 nm CQDs were used as catalyst, the final yields in aldol condensation were achieved in about 18 h for the first (red line) and second (blue line) cycle experiments and 22 h for the fifth (black line) cycle experiment. Moreover, the yield rate was slightly decreased along with the increase in cycles. For the other two kinds of catalysts (Figure 6b, >10 nm; Figure 6c, <4 nm), the similar catalytic effects were also observed in the recycle experiments. The above stability

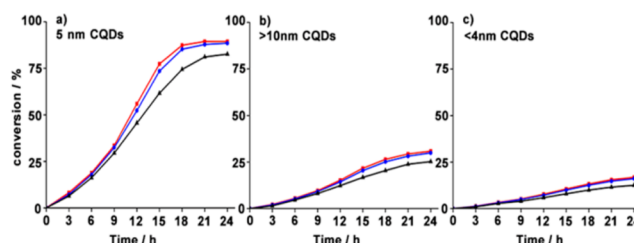


Figure 6. Kinetic plots track conversion over time for the first (red line), second (blue line), and fifth (black line) cycle experiments with different size CQDs as catalysts: (a) 5 nm; (b) >10 nm; and (c) <4 nm.

test results suggest that the CQD catalyst can be easily recycled as a heterogeneous catalyst with a long catalyst life.

In summary, we have demonstrated that CQDs (about 5 nm) were efficient photocatalysts for H-bond catalysis in the aldol condensation. CQDs showed excellent photoenhanced catalytic abilities (89% yield when 4-cyanobenzaldehyde is used) for H-bond catalysis with a series of aromatic aldehydes. Control catalytic experiments confirmed that the efficient electron-accepting properties of CQDs strengthened the O–H bond and activated the C=O bond of the 4-cyanobenzaldehyde, accelerating the aldol condensation. Our findings offer a novel approach for designing and fabricating the next generation of high-performance H-bond catalysts.

■ ASSOCIATED CONTENT

📄 Supporting Information

Preparation and characterization results of CQDs, FT-IR spectra of benzaldehyde mix with CQDs, luminescence decays of CQDs. This information is available free of charge via the Internet at <http://pubs.acs.org/>.

■ AUTHOR INFORMATION

Corresponding Authors

*E-mail: zhkang@suda.edu.cn.

*E-mail: yangl@suda.edu.cn.

Author Contributions

Y.H. and H.H. contributed equally to this work.

Notes

The authors declare no competing financial interest.

■ ACKNOWLEDGMENTS

This work is supported by the National Basic Research Program of China (973 Program) (No. 2012CB825800, 2013CB932702), National Natural Science Foundation of China (NSFC) (No. 51132006), a project funded by the Priority Academic Program Development of Jiangsu Higher Education Institutions (PAPD), a Suzhou Planning Project of Science and Technology (ZXG2012028).

■ REFERENCES

- (1) Knowles, R. R.; Jacobsen, E. N. *Proc. Natl. Acad. Sci. U.S.A.* **2010**, *107*, 20678–20685.
- (2) Pihko, P. M. *Angew. Chem., Int. Ed.* **2004**, *43*, 2062–2064.
- (3) Dalko, P. I.; Moisan, L. *Angew. Chem., Int. Ed.* **2004**, *43*, 5138–5175.
- (4) Akiyama, T.; Itoh, J.; Yokota, K.; Fuchibe, K. *Angew. Chem., Int. Ed.* **2004**, *43*, 1566–1568.
- (5) Gondi, V. B.; Gravel, M.; Rawal, V. H. *Org. Lett.* **2005**, *7*, 5657–5660.

- (6) Sigman, M. S.; Vachal, P.; Jacobsen, E. N. *Angew. Chem., Int. Ed.* **2000**, *39*, 1279–1281.
- (7) Okino, T.; Hoashi, Y.; Takemoto, Y. *J. Am. Chem. Soc.* **2003**, *125*, 12672–12673.
- (8) Nugent, B. M.; Yoder, R. A.; Johnston, J. N. *J. Am. Chem. Soc.* **2004**, *126*, 3418–3419.
- (9) Uraguchi, D.; Terada, M. *J. Am. Chem. Soc.* **2004**, *126*, 5356–5367.
- (10) Huang, Y.; Unni, A. K.; Thadani, A. N.; Rawal, V. H. *Nature* **2003**, *424*, 146.
- (11) Unni, A. K.; Takenaka, N.; Yamamoto, H.; Rawal, V. H. *J. Am. Chem. Soc.* **2005**, *127*, 1336–1337.
- (12) (a) Hoashi, Y.; Okino, T.; Takemoto, Y. *Angew. Chem., Int. Ed.* **2005**, *117*, 4100–4103. (b) Zeidan, R. K.; Hwang, S.-J.; Davis, M. E. *Angew. Chem., Int. Ed.* **2006**, *45*, 6332–6335. (c) Zeidan, R. K.; Davis, M. E. *J. Catal.* **2007**, *247*, 379–382. (d) Solin, N.; Han, L.; Che, S.; Terasaki, O. *Catal. Commun.* **2009**, *10*, 1386–1389.
- (13) Rajaram, S.; Sigman, M. S. *Org. Lett.* **2005**, *7*, 5473–5475.
- (14) Sigman, M. S.; Vachal, P.; Jacobsen, E. N. *Angew. Chem., Int. Ed.* **2000**, *112*, 1336–1338.
- (15) Wenzel, A. G.; Jacobsen, E. N. *J. Am. Chem. Soc.* **2002**, *124*, 12964–12965.
- (16) Akiyama, T.; Itoh, J.; Yokota, K.; Fuchibe, K. *Angew. Chem., Int. Ed.* **2004**, *116*, 1592–1594.
- (17) McGilvra, J. D.; Unni, A. K.; Modi, K.; Rawal, V. H. *Angew. Chem., Int. Ed.* **2006**, *45*, 6130–6133.
- (18) Doyle, A. G.; Jacobsen, E. N. *Chem. Rev.* **2007**, *107*, 5713–5743.
- (19) Kelly, T. R.; Meghani, P.; Ekkundi, V. S. *Tetrahedron Lett.* **1990**, *31*, 3381–3384.
- (20) Momiyama, N.; Yamamoto, H. *J. Am. Chem. Soc.* **2005**, *127*, 1080–1081.
- (21) Niu, F.; Wu, J. Y.; Zhang, L. S.; Li, P.; Zhu, J. F.; Wu, Z. Y.; Wang, C. R.; Song, W.-G. *ACS Catal.* **2011**, *1*, 1158–1161.
- (22) McDougal, N. T.; Schaus, S. E. *J. Am. Chem. Soc.* **2003**, *125*, 12094–12095.
- (23) Niu, F.; Liu, C. C.; Cui, Z. M.; Zhai, J.; Jiang, L.; Song, W.-G. *Chem. Commun.* **2008**, *44*, 2803–2805.
- (24) Niu, F.; Zhai, J.; Jiang, L.; Song, W.-G. *Chem. Commun.* **2009**, *45*, 4738–4740.
- (25) Niu, F.; Zhang, L.; Luo, S. Z.; Song, W.-G. *Chem. Commun.* **2010**, *46*, 1109–1111.
- (26) Li, H. T.; He, X. D.; Kang, Z. H.; Huang, H.; Liu, Y.; Liu, J. L.; Lian, S. Y.; Tsang, C. H. A.; Yang, X. B.; Lee, S. T. *Angew. Chem., Int. Ed.* **2010**, *49*, 4430–4434.
- (27) Zhang, H. C.; Huang, H.; Ming, H.; Li, H. T.; Zhang, L. L.; Liu, Y.; Kang, Z. H. *J. Mater. Chem.* **2012**, *22*, 10501–10506.
- (28) Zhang, H. C.; Ming, H.; Lian, S. Y.; Huang, H.; Li, H. T.; Zhang, L. L.; Liu, Y.; Kang, Z. H.; Lee, S. T. *Dalton Trans.* **2011**, *40*, 10822–10825.
- (29) Han, X.; Han, Y. Z.; Huang, H.; Zhang, H. C.; Zhang, X.; Liu, R. H.; Liu, Y.; Kang, Z. H. *Dalton Trans.* **2013**, *42*, 10380–10383.
- (30) Li, H. T.; Liu, R. H.; Liu, Y.; Huang, H.; Yu, H.; Ming, H.; Lian, S. Y.; Lee, S. T.; Kang, Z. H. *J. Mater. Chem.* **2012**, *22*, 17470–17475.
- (31) (a) Hohl, H.; Stumm, W. *J. Colloid Interface Sci.* **1976**, *55*, 281–288. (b) Crocker, M.; Herold, R. H. M.; Sonnemans, M. H. W.; Emeis, C. A.; Wilson, A. E.; Vandermoelen, J. N. *J. Phys. Chem.* **1993**, *97*, 432–439. (c) Sengoku, T.; Takemura, T.; Fukasawa, E.; Hayakawa, I.; Kigoshi, H. *Tetrahedron Lett.* **2009**, *50*, 325–328.
- (32) Zhao, L.; Sun, Z.-Z.; Ma, J. *Environ. Sci. Technol.* **2009**, *43*, 4157–4163.
- (33) McKeen, J. C.; Yan, Y. S.; Davis, M. E. *Chem. Mater.* **2008**, *20*, 3791–3793.
- (34) Mukhopadhyay, A.; Mukherjee, M.; Pandey, P.; Samanta, A. K.; Bandyopadhyay, B.; Chakraborty, T. *J. Phys. Chem. A* **2009**, *113*, 3078–3087.
- (35) van der Veken, B. J.; Herrebout, W. A.; Szostak, R.; Shchepkin, D. N.; Havlas, Z.; Hobza, P. *J. Am. Chem. Soc.* **2001**, *123*, 12290–12293.
- (36) Chocholoušová, J.; Špirko, V.; Hobza, P. *Phys. Chem. Chem. Phys.* **2004**, *6*, 37–41.
- (37) Wang, X.; Cao, L.; Lu, F. S.; Meziani, M. J.; Li, H. T.; Qi, G.; Zhou, B.; Harruff, B. A.; Kermarrec, F.; Sun, Y.-P. *Chem. Commun.* **2009**, 3774–3776.
- (38) Rehm, J. M.; Mclendon, G. L.; Fauchet, P. M. *J. Am. Chem. Soc.* **1996**, *118*, 4490–4491.
- (39) Li, H. T.; Liu, R. H.; Lian, S. Y.; Liu, Y.; Huang, H.; Kang, Z. H. *Nanoscale* **2013**, *5*, 3289–3297.
- (40) Chen, X.; Brauman, J. I. *J. Am. Chem. Soc.* **2008**, *130*, 15038–15046.
- (41) Kubota, Y.; Yamaguchi, H.; Yamada, T.; Inagaki, S.; Sugi, Y.; Tatsumi, T. *Top. Catal.* **2010**, *53*, 492–499.
- (42) Alabugin, I. V.; Manoharan, M.; Peabody, S.; Weinhold, F. *J. Am. Chem. Soc.* **2003**, *125*, 5973–5987.
- (43) Joseph, J.; Jemmis, E. D. *J. Am. Chem. Soc.* **2007**, *129*, 4620–4632.